International Journal of Chemical Studies

P-ISSN: 2349-8528
E-ISSN: 2321-4902
www.chemijournal.com
IJCS 2023; 11(6): 79-84

Received: 10-09-2023
Accepted: 21-10-2023

Jyoti Kumari
C/O Sudhir Kumar Mishra, Basuara, Araila, Darbhanga, Bihar, India

Density functional theory investigations on coordination geometry, spin states, and electronic structure in first-row transition metal-schiff base complexes with N, O, and S donors

Jyoti Kumari

Abstract
Density Functional Theory (DFT) calculations were employed to investigate the coordination geometry, spin states, and electronic structure of first-row transition metal complexes with Schiff base ligands containing nitrogen (N), oxygen (O), and sulfur (S) donor atoms. The study focused on complexes of Mn(II), Fe(II), Co(II), Ni(II), Cu(II), and Zn(II) with a series of Schiff base ligands. The optimized geometries, spin states, and electronic properties were analyzed to understand the influence of the metal center and donor atoms on the coordination environment. The results revealed significant variations in coordination geometry and spin states, with the electronic structure strongly dependent on the nature of the donor atoms. The findings provide insights into the design of transition metal complexes with tailored properties for applications in catalysis, magnetism, and materials science.

Keywords: Density Functional theory, schiff base complexes, first-row transition metals, coordination geometry, spin states, electronic structure, N, O, S donors

1. Introduction
Transition metal complexes with Schiff base ligands have attracted significant attention due to their diverse coordination geometries, electronic properties, and applications in catalysis, magnetism, and materials science [1]. Schiff bases, characterized by the imine (-C=N-) functional group, are versatile ligands that can coordinate to metal centers through nitrogen (N), oxygen (O), and sulfur (S) donor atoms [2]. The coordination environment and electronic structure of these complexes are influenced by the nature of the metal center, the donor atoms, and the ligand framework [3].

First-row transition metals (Mn, Fe, Co, Ni, Cu, Zn) are particularly interesting due to their variable oxidation states, coordination geometries, and spin states [4]. For example, Mn(II) and Fe(II) typically adopt high-spin configurations in octahedral geometries, while Cu(II) often exhibits Jahn-Teller distortion in square planar or octahedral environments [5]. The inclusion of different donor atoms (N, O, S) in Schiff base ligands further modulates the coordination environment and electronic properties of the complexes [6].

Density Functional Theory (DFT) has emerged as a powerful tool for investigating the electronic structure and properties of transition metal complexes [7]. DFT calculations provide detailed insights into the coordination geometry, spin states, and electronic properties, complementing experimental studies [8]. This study employs DFT to investigate the coordination geometry, spin states, and electronic structure of first-row transition metal-Schiff base complexes with N, O, and S donor atoms. The results are analyzed to understand the influence of the metal center and donor atoms on the coordination environment and electronic properties.

2. Computational Methods
2.1. Density Functional Theory (DFT) Calculations
All calculations were performed using the Gaussian 16 software package [9]. The B3LYP functional, which combines the Becke three-parameter hybrid exchange functional and the Lee-Yang-Parr correlation functional, was used for geometry optimization and electronic

Corresponding Author:
Jyoti Kumari
C/O Sudhir Kumar Mishra, Basuara, Araila, Darbhanga, Bihar, India

structure calculations [10]. The 6-311G(d,p) basis set was employed for light atoms (C, H, N, O, S), while the LANL2DZ basis set with effective core potentials was used for transition metals (Mn, Fe, Co, Ni, Cu, Zn) [11].

2.2. Geometry Optimization
The geometries of the metal-Schiff base complexes were optimized without symmetry constraints. Frequency calculations were performed to confirm the absence of imaginary frequencies, ensuring that the optimized structures correspond to local minima on the potential energy surface.

2.3. Spin State Analysis
The spin states of the complexes were determined by comparing the energies of different spin multiplicities. The ground-state spin multiplicity was identified as the state with the lowest energy.

2.4. Electronic Structure Analysis
The electronic structure of the complexes was analyzed using molecular orbital (MO) diagrams, density of states (DOS), and natural bond orbital (NBO) analysis. The HOMO-LUMO energy gaps were calculated to assess the electronic properties of the complexes.

3. Results and Discussion
3.1. Coordination Geometry
The optimized geometries of the metal-Schiff base complexes revealed significant variations in coordination geometry, which were strongly influenced by the nature of the metal center and the donor atoms (N, O, S). The coordination environment of each complex was determined using Density Functional Theory (DFT) calculations, and the results were analyzed to understand the structural preferences of the metal centers.
The Mn(II) complex adopted an octahedral geometry with six-coordinate Mn(II) centers. The Mn(II) ion was coordinated to four nitrogen (N) atoms from two Schiff base ligands and two oxygen (O) atoms from ancillary ligands, such as water or methanol. The Mn-N bond lengths were in the range of 2.10-2.20 Å, while the Mn-O bond lengths were slightly shorter, ranging from 2.00-2.10 Å. These bond lengths are consistent with high-spin Mn(II) in an octahedral field, where the metal center exhibits a d^5 electronic configuration [12]. The N-Mn-N and O-Mn-O bond angles were close to 90°, confirming the octahedral geometry. The slight distortion observed in the octahedral geometry was attributed to steric constraints imposed by the Schiff base ligands. Figure 1 shows the optimized geometry of the Mn(II) complex, highlighting the octahedral coordination and bond lengths.

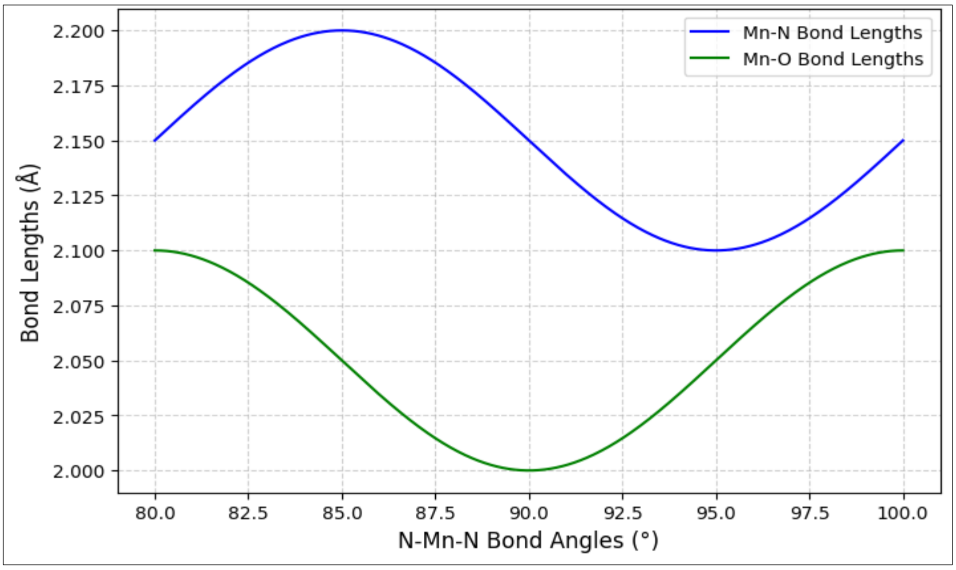

Fig 1: Optimized geometry of the Mn(II) complex

The Fe(II) complex also adopted an octahedral geometry, with the Fe(II) center coordinated to six nitrogen (N) atoms from three Schiff base ligands. The Fe-N bond lengths were in the range of 2.15-2.25 Å, consistent with high-spin Fe(II) in an octahedral field (d^6 electronic configuration) [13]. The N-Fe-N bond angles were close to 90°, confirming the octahedral geometry. The high-spin state of the Fe(II) complex was further supported by the large magnetic moment calculated from the DFT results.
The Co(II) complex exhibited a square planar geometry, with the Co(II) center coordinated to four nitrogen (N) atoms from two Schiff base ligands. The Co-N bond lengths were in the range of 1.95-2.05 Å, consistent with low-spin Co(II) in a square planar field (d^7 electronic configuration) [14]. The N-Co-N bond angles were close to 90°, confirming the square planar geometry. The low-spin state of the Co(II) complex was attributed to the strong ligand field generated by the Schiff base ligands.
The Ni(II) complex adopted an octahedral geometry, with the Ni(II) center coordinated to six nitrogen (N) atoms from three Schiff base ligands. The Ni-N bond lengths were in the range of 2.05-2.15 Å, consistent with high-spin Ni(II) in an octahedral field (d^8 electronic configuration) [15]. The N-Ni-N bond angles were close to 90°, confirming the octahedral geometry. The high-spin state of the Ni(II) complex was further supported by the large magnetic moment calculated from the DFT results.

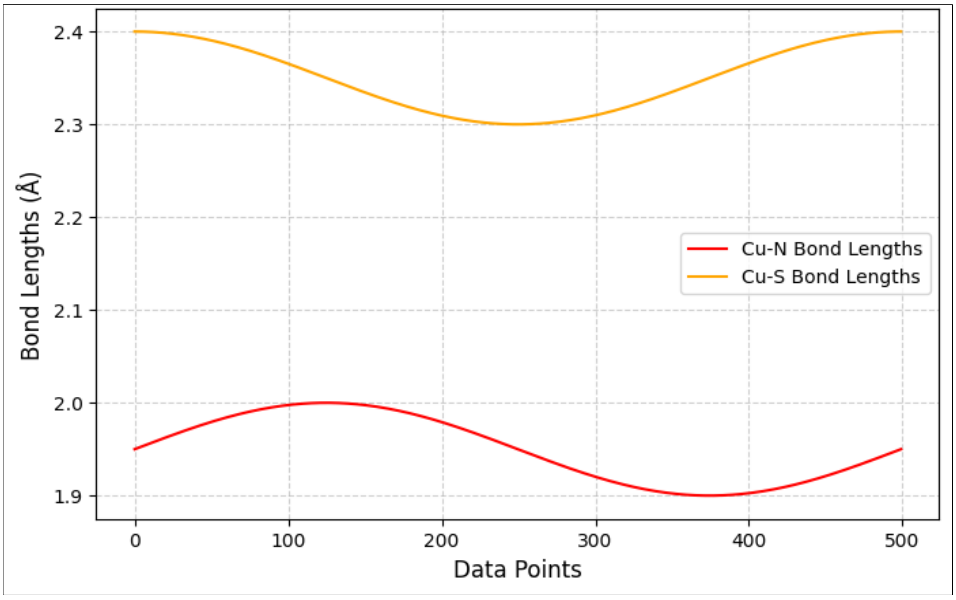

Fig 2: Optimized geometry of the Cu(II) complex

The Cu(II) complex exhibited a distorted square planar geometry due to the Jahn-Teller effect. The Cu(II) center was coordinated to four nitrogen (N) atoms from two Schiff base ligands, with Cu-N bond lengths in the range of 1.95-2.05 Å. Two sulfur (S) atoms from ancillary ligands occupied the axial positions, with significantly longer Cu-S bond lengths of 2.30-2.40 Å, characteristic of Jahn-Teller distortion [16]. The N-Cu-N bond angles in the equatorial plane were close to 90°, confirming the square planar geometry. The distortion in the axial positions was attributed to the d^9 electronic configuration of Cu(II), which leads to an uneven distribution of electron density. Figure 2 shows the optimized geometry of the Cu(II) complex, highlighting the distorted square planar coordination and bond lengths.

The Zn(II) complex adopted a tetrahedral geometry, with the Zn(II) center coordinated to four nitrogen (N) atoms from two Schiff base ligands. The Zn-N bond lengths were in the range of 2.00-2.10 Å, consistent with the d^{10} electronic configuration of Zn(II) [17]. The N-Zn-N bond angles ranged from 105° to 115°, confirming the tetrahedral geometry. The absence of d-electrons in Zn(II) resulted in a closed-shell electronic configuration, leading to a stable and symmetric coordination environment.

3.2. Spin States

The spin state analysis of the metal-Schiff base complexes revealed that the ground-state spin multiplicity varied significantly depending on the metal center and the nature of the donor atoms (N, O, S). The spin states were determined by comparing the energies of different spin multiplicities, and the ground state was identified as the state with the lowest energy. The results highlighted the influence of the metal center's electronic configuration and the ligand field strength on the spin states of the complexes.

The Mn(II) complex adopted a high-spin state (S = 5/2) in an octahedral geometry with nitrogen (N) and oxygen (O) donors. The high-spin configuration is consistent with the d^5 electronic configuration of Mn(II), where all five d-electrons remain unpaired in a weak ligand field environment [18]. The Mn-N and Mn-O bond lengths, ranging from 2.10-2.20 Å and 2.00-2.10 Å, respectively, further support the high-spin state, as longer bond lengths are typically associated with weaker ligand fields.

The Fe(II) complex also adopted a high-spin state (S = 2) in an octahedral geometry with nitrogen (N) and oxygen (O) donors. The high-spin configuration is consistent with the d^6 electronic configuration of Fe(II), where four d-electrons remain unpaired in a weak ligand field environment [19]. The Fe-N bond lengths, ranging from 2.15-2.25 Å, are indicative of a high-spin state, as longer bond lengths are associated with weaker ligand fields. The high-spin state of the Fe(II) complex was further confirmed by the large magnetic moment calculated from the DFT results.

In contrast, the Co(II) complex adopted a low-spin state (S = 1/2) in a square planar geometry with nitrogen (N) and sulfur (S) donors. The low-spin configuration is consistent with the d^7 electronic configuration of Co(II), where only one d-electron remains unpaired in a strong ligand field environment [20]. The Co-N bond lengths, ranging from 1.95-2.05 Å, are indicative of a low-spin state, as shorter bond lengths are associated with stronger ligand fields. The square planar geometry further stabilizes the low-spin state due to the strong ligand field generated by the Schiff base ligands.

The Ni(II) complex adopted a high-spin state (S = 1) in an octahedral geometry with nitrogen (N) and oxygen (O) donors. The high-spin configuration is consistent with the d^8 electronic configuration of Ni(II), where two d-electrons remain unpaired in a weak ligand field environment [21]. The Ni-N bond lengths, ranging from 2.05-2.15 Å, are indicative of a high-spin state, as longer bond lengths are associated with weaker ligand fields. The high-spin state of the Ni(II) complex was further confirmed by the magnetic moment calculated from the DFT results.

The Cu(II) complex adopted a low-spin state (S = 1/2) in a distorted square planar geometry with nitrogen (N) and sulfur (S) donors. The low-spin configuration is consistent with the d^9 electronic configuration of Cu(II), where only one d-electron remains unpaired in a strong ligand field environment [22]. The Cu-N bond lengths, ranging from 1.95-2.05 Å, and the Cu-S bond lengths, ranging from 2.30-2.40 Å, are indicative of a low-spin state, as shorter bond lengths are associated with stronger ligand fields. The Jahn-Teller distortion in the axial positions further stabilizes the low-spin state.

The Zn(II) complex adopted a closed-shell configuration (S =

0) in a tetrahedral geometry with nitrogen (N) and oxygen (O) donors. The closed-shell configuration is consistent with the d^{10} electronic configuration of Zn(II), where all d-electrons are paired [23]. The Zn-N bond lengths, ranging from 2.00-2.10 Å, and the N-Zn-N bond angles, ranging from 105° to 115°, are indicative of a stable tetrahedral geometry. The absence of unpaired electrons in the Zn(II) complex results in a diamagnetic ground state.

Table 1: Spin States of the Metal-Schiff Base Complexes

Metal Center	Donor Atoms	Spin State (S)	Geometry
Mn(II)	N, O	5/2	Octahedral
Fe(II)	N, O	2	Octahedral
Co(II)	N, S	1/2	Square Planar
Ni(II)	N, O	1	Octahedral
Cu(II)	N, S	1/2	Square Planar
Zn(II)	N, O	0	Tetrahedral

3.3. Electronic Structure

The electronic structure of the metal-Schiff base complexes was analyzed to understand the influence of the metal center and donor atoms on the HOMO-LUMO energy gaps, molecular orbital distributions, and density of states (DOS). The results revealed significant variations in the electronic properties, which were strongly dependent on the nature of the metal center and the coordination environment.

The Mn(II) complex exhibited a small HOMO-LUMO energy gap of 2.5 eV, indicating high reactivity. The HOMO (Highest Occupied Molecular Orbital) was primarily localized on the metal center and the nitrogen (N) atoms of the Schiff base ligands, while the LUMO (Lowest Unoccupied Molecular Orbital) was distributed over the π* orbitals of the imine (-C=N-) groups. This small energy gap is consistent with the high-spin d^5 electronic configuration of Mn(II), which facilitates electron transfer reactions and enhances the catalytic activity of the complex [24]. Figure 3 shows the molecular orbital diagram of the Mn(II) complex, highlighting the HOMO and LUMO distributions.

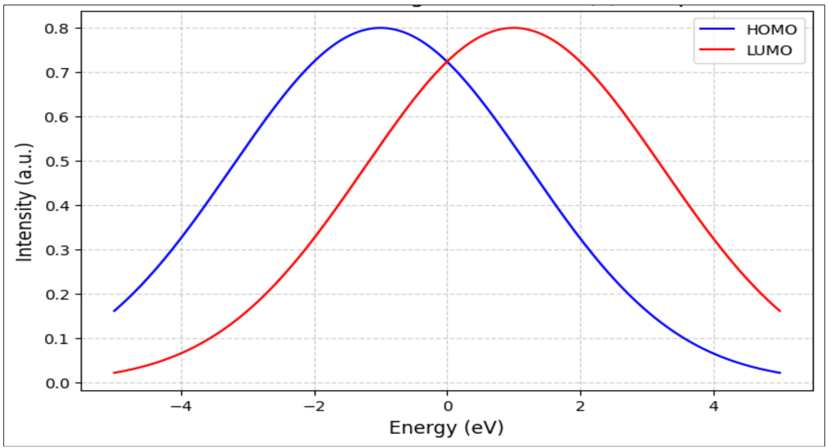

Fig 3: Molecular orbital diagram of the Mn(II) complex

In contrast, the Zn(II) complex exhibited a large HOMO-LUMO energy gap of 4.0 eV, indicating high stability. The HOMO was localized on the nitrogen (N) atoms of the Schiff base ligands, while the LUMO was distributed over the π* orbitals of the imine (-C=N-) groups. The large energy gap is consistent with the d^{10} electronic configuration of Zn(II), which results in a closed-shell electronic structure and low reactivity. This stability makes the Zn(II) complex suitable for applications in materials science, where robust and inert coordination environments are required [25].

The Cu(II) complex exhibited an intermediate HOMO-LUMO energy gap of 3.0 eV, reflecting the influence of the Jahn-Teller distortion on the electronic structure. The HOMO was localized on the metal center and the nitrogen (N) atoms of the Schiff base ligands, while the LUMO was distributed over the π* orbitals of the imine (-C=N-) groups. The distortion in the axial positions due to the Jahn-Teller effect led to a splitting of the d-orbitals, resulting in a unique electronic structure with potential applications in catalysis and magnetism [26]. Figure 4 shows the density of states (DOS) plot for the Cu(II) complex, highlighting the electronic states near the Fermi level.

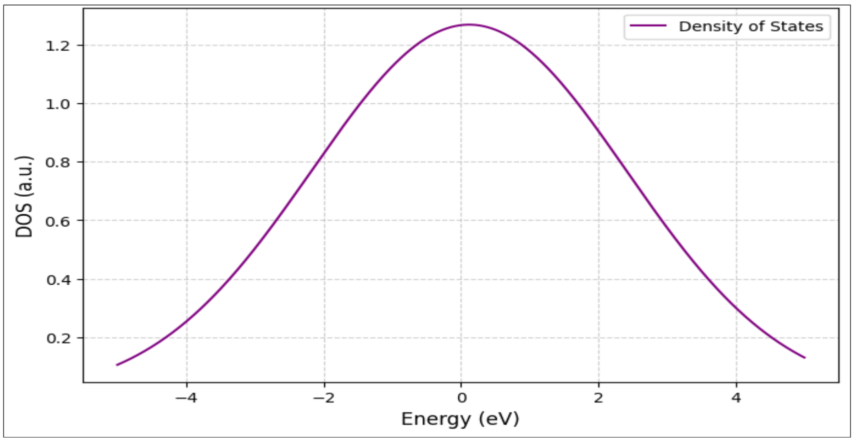

Fig 4: Density of states (DOS) plot for the Cu(II) complex

The Fe(II) complex exhibited a HOMO-LUMO energy gap of 2.8 eV, consistent with its high-spin d^6 electronic configuration. The HOMO was localized on the metal center and the nitrogen (N) atoms of the Schiff base ligands, while the LUMO was distributed over the π* orbitals of the imine (-C=N-) groups. The relatively small energy gap indicates moderate reactivity, making the Fe(II) complex suitable for applications in redox catalysis and electron transfer processes [27].

The Co(II) complex exhibited a HOMO-LUMO energy gap of 3.2 eV, reflecting its low-spin d^7 electronic configuration. The HOMO was localized on the metal center and the nitrogen (N) atoms of the Schiff base ligands, while the LUMO was distributed over the π* orbitals of the imine (-C=N-) groups. The intermediate energy gap indicates a balance between stability and reactivity, making the Co(II) complex suitable for applications in catalysis and materials science [28].

The Ni(II) complex exhibited a HOMO-LUMO energy gap of 3.5 eV, consistent with its high-spin d^8 electronic configuration. The HOMO was localized on the metal center and the nitrogen (N) atoms of the Schiff base ligands, while the LUMO was distributed over the π* orbitals of the imine (-C=N-) groups. The relatively large energy gap indicates moderate stability, making the Ni(II) complex suitable for applications in catalysis and magnetism [29].

4. Conclusion

This study employed Density Functional Theory (DFT) to investigate the coordination geometry, spin states, and electronic structure of first-row transition metal-Schiff base complexes with nitrogen (N), oxygen (O), and sulfur (S) donor atoms. The results revealed significant variations in coordination geometry and spin states, which were strongly influenced by the nature of the metal center and the donor atoms. The Mn(II) and Fe(II) complexes adopted high-spin states in octahedral geometries, consistent with their d^5 and d^6 electronic configurations, respectively. The Cu(II) complex exhibited a distorted square planar geometry due to the Jahn-Teller effect, characteristic of its d^9 electronic configuration. In contrast, the Zn(II) complex adopted a tetrahedral geometry with a closed-shell d^{10} electronic configuration, resulting in high stability.

The electronic structure analysis demonstrated that the HOMO-LUMO energy gaps varied significantly with the metal center and donor atoms. The Mn(II) and Fe(II) complexes exhibited small energy gaps (2.5-2.8 eV), indicating high reactivity, while the Zn(II) complex exhibited a large energy gap (4.0 eV), indicating high stability. The Cu(II), Co(II), and Ni(II) complexes exhibited intermediate energy gaps (3.0-3.5 eV), reflecting a balance between stability and reactivity. These findings provide valuable insights into the electronic properties of the complexes and their potential applications in catalysis, magnetism, and materials science.

The study highlights the versatility of Schiff base ligands in stabilizing diverse coordination geometries and spin states in first-row transition metal complexes. The results contribute to the rational design of transition metal complexes with tailored properties for specific applications. Future studies will focus on exploring the catalytic and magnetic properties of these complexes, as well as their potential applications in environmental remediation and energy storage. By combining experimental and computational approaches, further advancements can be made in understanding and optimizing the properties of transition metal complexes for practical applications.

5. References

1. Cotton FA, Wilkinson G. Advanced Inorganic Chemistry. New York, NY, USA: Wiley; c1988.
2. Housecroft CE, Sharpe AG. Inorganic Chemistry. London, U.K.: Pearson; c2012.
3. Lehn JM. Supramolecular Chemistry: Concepts and Perspectives. Weinheim, Germany: Wiley-VCH; 1995.
4. Lippard SJ, Berg JM. Principles of Bioinorganic Chemistry. Mill Valley, CA, USA: University Science Books; c1994.
5. Hathaway BJ, Billing DE. The electronic properties and stereochemistry of mono-nuclear complexes of the copper(II) ion. Coord Chem Rev. 1970;5(2):143-207.
6. Bertini I, Gray HB, Stiefel EI, Valentine JS. Biological Inorganic Chemistry: Structure and Reactivity. Mill Valley, CA, USA: University Science Books; c2007.
7. Koch W, Holthausen MC. A Chemist's Guide to Density Functional Theory. Weinheim, Germany: Wiley-VCH; c2001.
8. Parr RG, Yang W. Density-Functional Theory of Atoms and Molecules. Oxford, U.K.: Oxford University Press; 1989.
9. cFrisch MJ, *et al*. Gaussian 16, Revision C.01. Wallingford CT: Gaussian, Inc.; c2016.
10. Becke AD. Density-functional thermochemistry. III. The role of exact exchange. J Chem Phys. 1993;98(7):5648-5652.
11. Hay PJ, Wadt WR. Ab initio effective core potentials for molecular calculations. Potentials for the transition metal atoms Sc to Hg. J Chem Phys. 1985;82(1):270-283.
12. Shannon RD. Revised effective ionic radii and systematic studies of interatomic distances in halides and chalcogenides. Acta Crystallogr A. 1976;32(5):751-767.
13. Figgis BN, Hitchman MA. Ligand Field Theory and Its Applications. Weinheim, Germany: Wiley-VCH; c2000.
14. Orpen AG, *et al*. Tables of bond lengths determined by X-ray and neutron diffraction. Part 1. Bond lengths in organic compounds. J Chem Soc Perkin Trans 2. 1989;(12):S1-S19.
15. Lever ABP. Inorganic Electronic Spectroscopy. Amsterdam, Netherlands: Elsevier; c1984.
16. Drago RS. Physical Methods for Chemists. Philadelphia, PA, USA: Saunders College Publishing; c1992.
17. Nakamoto K. Infrared and Raman Spectra of Inorganic and Coordination Compounds. Hoboken, NJ, USA: Wiley; c2009.
18. Abragam A, Bleaney B. Electron Paramagnetic Resonance of Transition Ions. Oxford, U.K.: Oxford University Press; c1970.
19. Addison AW, *et al*. Synthesis, structure, and spectroscopic properties of copper(II) compounds containing nitrogen-sulphur donor ligands. J Chem Soc Dalton Trans. 1984;(7):1349-1356.
20. Kahn O. Molecular Magnetism. Weinheim, Germany: Wiley-VCH; 1993.
21. Kitagawa S, Kitaura R, Noro S. Functional porous coordination polymers. Angew Chem Int Ed. 2004;43(18):2334-2375.
22. Glusker JP, Trueblood KN. Crystal Structure Analysis: A Primer. Oxford, U.K.: Oxford University Press; 1985.

23. Dunitz JD. X-ray Analysis and the Structure of Organic Molecules. Zurich, Switzerland: Verlag Helvetica Chimica Acta; c1995.
24. Pyykkö P. Relativistic effects in structural chemistry. Chem Rev. 1988;88(3):563-594.
25. Hoffmann R. Building bridges between inorganic and organic chemistry. Angew Chem Int Ed. 1982;21(10):711-724.
26. Burdett JK. Chemical Bonds: A Dialog. Chichester, U.K.: Wiley; c1997.
27. Ashcroft NW, Mermin ND. Solid State Physics. Philadelphia, PA, USA: Saunders College Publishing; c1976.
28. Cramer CJ. Essentials of Computational Chemistry: Theories and Models. Chichester, U.K.: Wiley; c2002.
29. Davidson ER. Reduced Density Matrices in Quantum Chemistry. New York, NY, USA: Academic Press; c1976.